EXPERIMENTAL NEUROLOGY **144,** 361–368 (1997)
ARTICLE NO. EN976413

Cholinergic Synapses in Human Cerebral Cortex: An Ultrastructural Study in Serial Sections

John F. Smiley,* Frank Morrell,†,[1] and M. Marsel Mesulam*

**The Cognitive Neurology and Alzheimer's Disease Center, Northwestern University Medical School, Chicago, Illinois 60611; and †Department of Neurological Sciences, Rush Presbetyrian–St. Lukes Medical Center, Chicago, Illinois 60612*

Cholinergic axons in the human cerebral cortex were analyzed by electron microscopy. Choline acetyltransferase (ChAT) immunoreactivity was used to identify cholinergic axons in samples of anterior temporal lobe removed at surgery. A systematic survey of labeled axon varicosities, visualized in complete serial sections, showed that 67% of all varicosities formed identifiable synaptic specializations. These synapses were usually symmetric and quite small, often present in only one to two serial sections. However, an occasional synapse was asymmetric and larger, seen in five to seven serial sections. The postsynaptic processes at cholinergic synapses were often identified as spiny dendrites or spines. The existence of cholinergic axons in the human cerebral cortex has been demonstrated in numerous studies. Our findings provide the first ultrastructural evidence that these axons make synaptic contact with cortical neurons in the human brain.

INTRODUCTION

Cholinergic axons comprise probably the most abundant extrathalamic afferent system to the cerebral cortex. These projections arise from cell groups of the basal forebrain and are topographically organized, as demonstrated by tract tracing in rats and monkeys (17). Cholinergic axons are dense throughout the cerebral cortex, although they are comparatively more dense in limbic areas and in layers I–II in most areas (16).

In the cingulate cortex of the rat, Descarries and colleagues found that only 15% of cholinergic axon varicosities formed identifiable synapses (26). In prefrontal cortex of the monkey synapses were identified on 40% of cholinergic axon varicosities (20). These observations suggest that these axons might rely heavily on nonsynaptic volume transmission to mediate their postsynaptic effects, a conclusion that could have major implications for understanding the manner in which acetylcholine exerts its influence on cortical cholinoceptive neurons.

The aim of the present study was to determine to what extent descriptions of cholinergic synaptic interactions in other animals are valid in the human cerebral cortex. For this purpose, we used serial section electron microscopy in surgically removed temporal cortex to characterize the synaptic interactions and morphology of cholinergic axons. Particular attention was paid to the percentage of cholinergic axon varicosities which formed synapses, the morphology of their synaptic contacts and their cytoplasmic contents, and the types of neural processes receiving cholinergic synapses.

METHODS

Cerebral cortex from the anterior and anterior–lateral temporal pole was resected for the neurosurgical treatment of intractable epilepsy. Tissues from two patients were used in this study, chosen from four available samples because of their optimal ultrastructural preservation. One patient was a 20-year-old female with temporal lobe epilepsy and atrophy of the anterior hippocampus, and the second was a 10-year-old male with widespread epilepsy involving the temporal and frontal cortex. In both cases, Nissl-stained sections showed this to be granular neocortex. This tissue was obtained with the informed consent of the patients and was part of the specimen removed for pathological examination.

Within a few minutes of removal, tissue was thinly sliced to a thickness of about 1.0 cm and immersed in ice-cold fixative containing 4% paraformaldehyde, 0.08% glutaraldehyde, and 0.1 *M* phosphate buffer, pH 7.4. After overnight fixation at 4°C the tissue was rinsed and vibratome-sectioned to 40 μm thickness in ice-cold 0.1 *M* phosphate, pH 7.4. Sections were then transferred to plastic vials containing 30% sucrose in 0.1 *M* phosphate buffer, pH 7.4. The vials were frozen by immersion in liquid nitrogen and stored frozen until processing for immunocytochemistry.

Immunocytochemistry was done with the avidin–biotin–peroxidase complex (ABC) method (12) employ-

[1] Deceased, October 22, 1996.

0014-4886/97 $25.00

ing the Vectastain Elite ABC kit (Vector Laboratories, Burlingame, CA). The solution for antibody incubations contained 1% bovine serum albumin, 0.1% glycine, 0.3% normal goat serum, in 0.1 *M* phosphate buffer, pH 7.4. For light microscopy 0.3% Triton X-100 was added to enhance antibody penetration. To identify cholinergic axons, a rabbit polyclonal antibody to choline acetyltransferase (ChAT) was applied at a concentration of 1:2000 for 2 days at 4°C. This antibody was a gift of Lou Hersch, and its specificity has been described by German *et al.*, (8). After several rinses in phosphate buffer, the tissue was treated with the biotinylated secondary antibody for 2–4 h, rinsed several times, treated with the ABC complex for 1 h, and visualized using 0.04% diaminobenzidine or the Vectastain VIP-red chromogen. The VIP-red chromogen was used for electron microscopy because it gives a punctate reaction product which is easily identifiable, usually without obscuring the internal structures and synaptic specializations of labeled axons (31). For light microscopy, reaction with VIP-red or diaminobenzidine gave the same pattern of cortical axon labeling. Control sections incubated in a nonspecific rabbit IgG in place of anti-ChAT lacked labeled processes. After immunolabeling, tissue for electron microscopy was dehydrated, embedded in plastic, blocked, serial sectioned, and counterstained as previously described (24). Electron microscopy was done with a Jeol 100CX microscope equipped with a Z-axis tilting grid holder. Tissue for light microscopy was mounted on chrom–alum-coated glass slides and coverslipped in Permount.

Most of the electron microscopic analysis was done as a systematic survey of labeled axon varicosities in blocks from layers I and II from each surgical sample. In addition, some preliminary observations from layers II and V are described. The systematic survey of varicosities was done as previously described (24, 25). Briefly, when a labeled profile was encountered, its size and appearance were evaluated. If the labeling was too heavy to visualize cytoplasmic features, the process was ignored. If the process was judged to be greater than 0.2 μm in cross-section and contained synaptic vesicles, it was considered to be an axon varicosity, and its appearance was evaluated in all sections throughout the varicosity. Particular attention was given to the presence of clear and dense core vesicles and to synaptic specializations. When the varicosity was seen to form a synapse, the postsynaptic process was also evaluated in limited serial sections to look for identifying morphological features. In particular, the formation of spines or the presence of a spine apparatus was evaluated. Measurements of cholinergic varicosities were taken from the serial section where they reached their largest size, and measurements of postsynaptic processes were taken at the site of the cholinergic synapse. The shortest diameter of all profiles was measured, to avoid measuring the length of obliquely cut processes.

RESULTS

Light microscopic examination showed that ChAT immunoreactive axons formed a dense plexus of thin varicose axons (Fig. 1). These were present throughout the cortex but were significantly more dense in layer I. No immunoreactive cell bodies were seen.

Electron microscopy showed immunoreactivity in axon varicosities and intervaricose segments of unmyelinated axons. The thin intervaricose segments contained few scattered synaptic vesicles and occasional swellings due to the presence of mitochondria. Axon varicosities contained local accumulations of clear synaptic vesicles and mitochondria. Swellings were not considered varicosities when they lacked synaptic vesicles and contained only scant cytoplasm. Dense core vesicle were observed in 33% ($n = 14$) of the 42 labeled varicosities which were inspected in complete serial sections. Usually 1 to 5 dense core vesicles were present, although an occasional varicosity had a higher density (e.g., Fig. 2E). The presence of dense core vesicles did not correlate in any obvious way with other features of axon or synapse morphology. The average diameter of ChAT varicosities was 0.49 ± 0.18 μm (mean ± SD, $n = 42$).

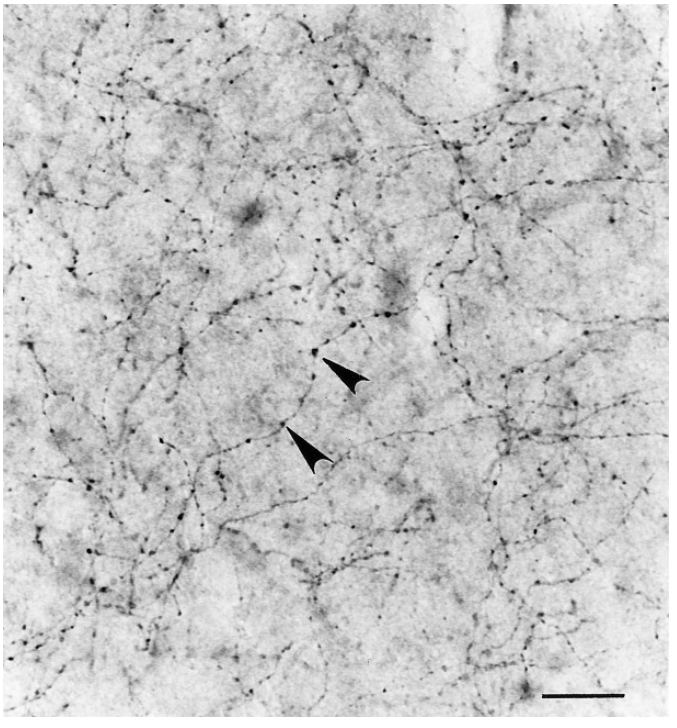

FIG. 1. ChAT immunoreactive axons in layer I of human cortex. Labeled axons were seen as a dense plexus of fine diameter axons which had many varicosities (arrowheads). Scale bar = 25 μm.

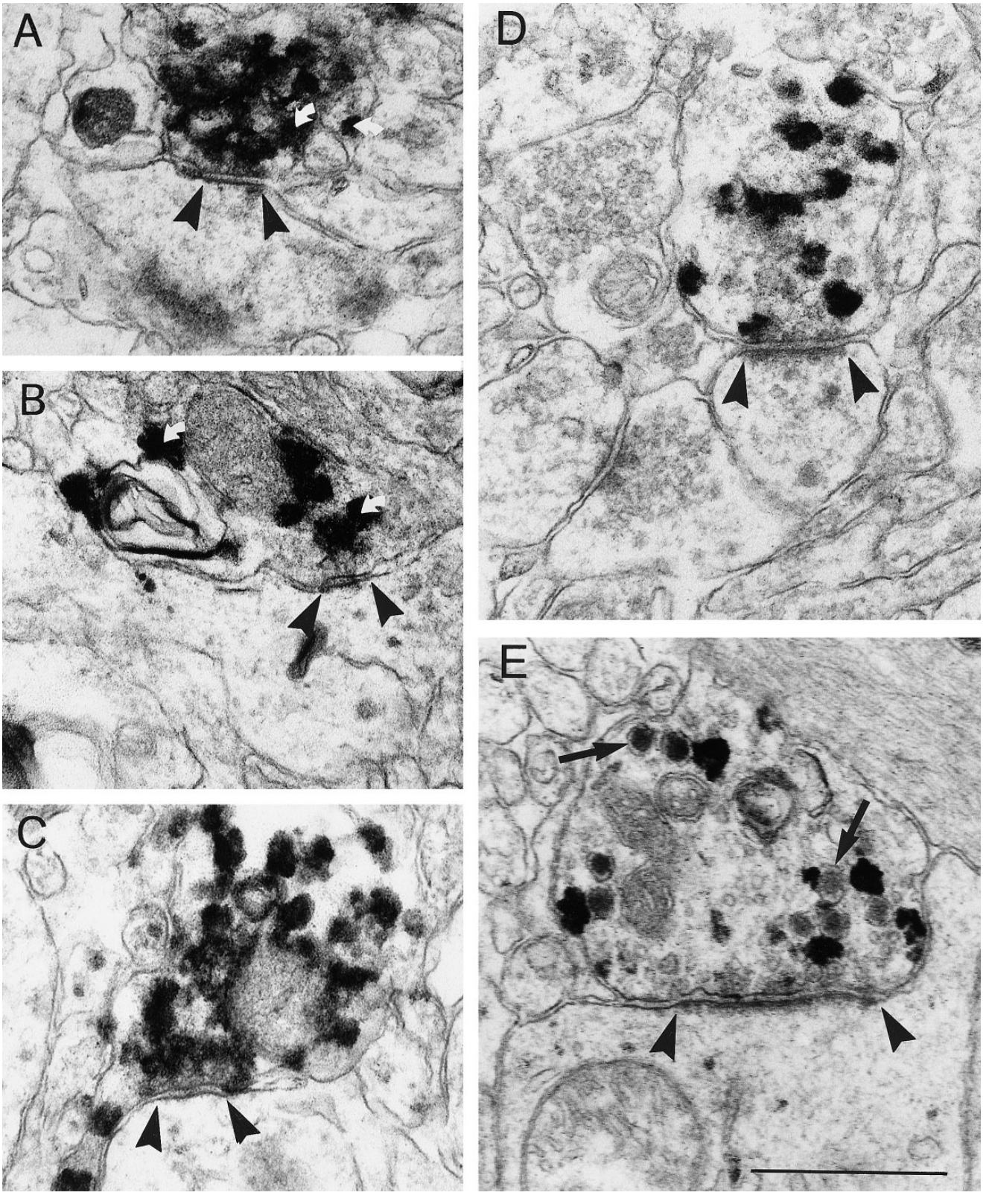

FIG. 2. Examples of symmetric (A–C) and asymmetric (D, E) cholinergic synapses (arrowheads) in human cortex. ChAT immunoreactivity is seen as dense floccular particles of "VIP-red" reaction product (white arrows). (A–C) Three varicosities of ChAT axons are seen forming symmetric synapses. In each case the synapse is shown in the serial section where it has reached its greatest diameter. (D) A labeled varicosity forming an asymmetric synapse. The postsynaptic process was identified as a spine head, with a spine apparatus and an unlabeled asymmetric synapse present in subsequent serial sections. (E) This labeled varicosity formed an unusually large asymmetric synapse onto a large dendritic shafts. The ChAT axon was also unusual because of the high density of dense core vesicles (arrows). Scale bar = 0.5 μm.

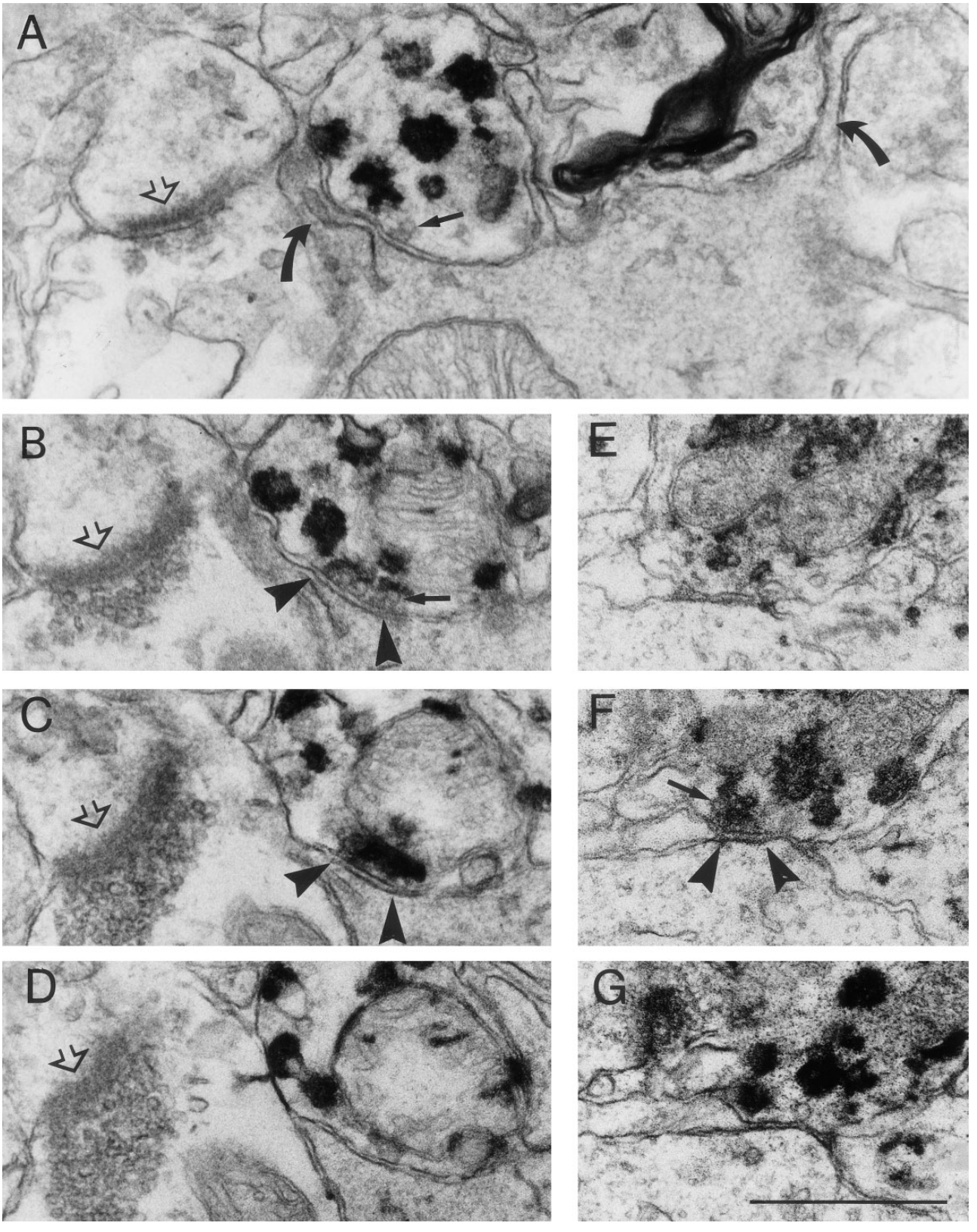

FIG. 3. Examples of especially small and subtle ChAT synapses, identified in serial sections. ChAT immunoreactivity is seen as dense floccular particles of "VIP-red" reaction product. (A–D) A ChAT axon is seen forming a small symmetric synapse onto the base of an apparent spine as it emerges from a dendrite. Numerous small apparent spines were seen emerging from this large dendrite (curved arrows in A). Seen

Synaptic interactions of ChAT axons were characterized in a systematic survey of immunolabeled varicosities from layers I and II. The presence of a synapse was determined by the presynaptic accumulation of clear vesicles, by the straightening and densification of the pre- and postsynaptic membranes, and by the widening of the space between these membranes. Of 42 varicosities surveyed in complete serial sections, 67% ($n = 28$) were seen to form clearly identifiable synaptic specializations. In many cases the membrane specializations were remarkably subtle and small, usually only identifiable in one or two sections (Figs. 2A–2C, 3, and 4). In some cases these were visualized only by tilting the grid. Even with tilting, it is likely that some synapses could not be identified because they were cut too tangentially or because the membrane densification was insufficient to allow confident synapse identification. Most identified synapses were classified as symmetrical because the densification of the postsynaptic membrane was not obviously greater than that of the presynaptic membrane (Figs. 2A–2C). A small number of synapses were classified as asymmetric because of the pronounced densification at their postsynaptic membranes (Figs. 2D and 2E). These synapses were larger than symmetric synapses and were seen in five to seven serial sections (Fig. 4). In one case the postsynaptic density was accompanied by subsynaptic dense bodies (not shown), similar to a previous observation in the rat motor cortex (11).

At the 28 synapses which were identified in this survey, the postsynaptic processes were characterized in limited numbers of serial sections. Most (71%, $n = 20$) were identified as dendritic shafts by the presence of mitochondria and microtubules. Postsynaptic dendritic shafts had a mean diameter of 0.67 ± .45 μm (mean ± SD). Many of these shafts ($n = 9$) were seen to form spines (e.g., Fig. 5), and three were 0.98 μm or more in diameter, suggesting that they were comparatively proximal dendrites of pyramidal cells. Two postsynaptic shafts had a high density of synapses, with approximately three to six synapses per micrometer, but these were not further characterized to determine if they might be nonspiny dendrites of interneurons. The remaining eight postsynaptic processes had the appearance of dendritic spines (diameter = 0.29 ± 0.13 μm). Two were spine heads, identified by the spine apparatus and nearby asymmetric synapse, and six

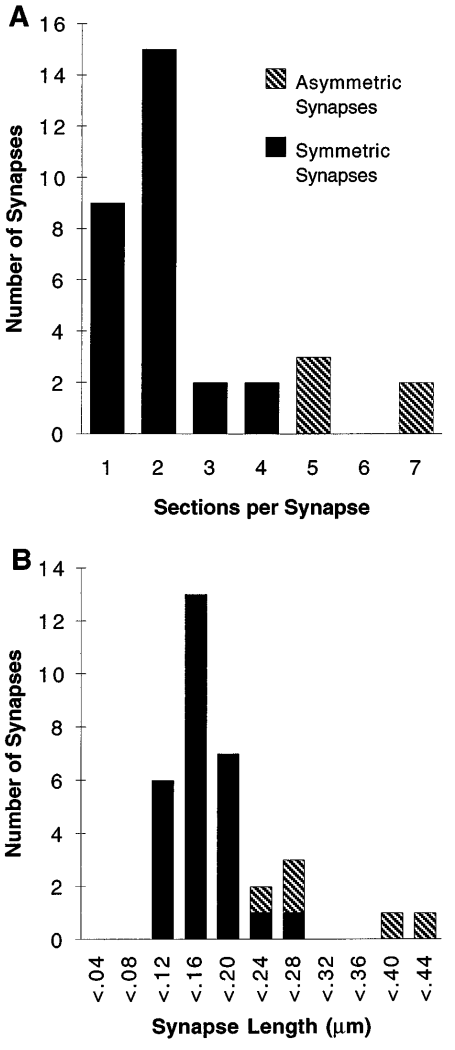

FIG. 4. Histograms showing the size of symmetric and asymmetric ChAT synapses. Synapse size is measure by two different methods. In A, the number of serial sections in which the synapses could be confidently identified is shown. Section thickness was approximately 0.07 μm. In B, the diameter of each synapse was measured on the serial section where it was largest. This sample of synapses includes 33 synapses; 5 are from preliminary observations in layers II and V and 28 are from systematically surveyed varicosities in layers I and II. The asymmetric synapse shown in Fig. 2E was larger than 0.44 μm in diameter, but was not included here because complete serial sections through it were not available. The diameter (mean ± SD) of this total sample of synapses was 2.5 ± 1.7 sections or 0.16 ± 0.08 μm. The diameter of symmetric synapses only was 1.9 ± 0.09 sections or 0.14 ± 0.03 μm.

nearby is an unlabeled asymmetric synapse onto a dendritic spine (open arrows). The ChAT synapse is identified by the presence of presynaptic vesicles (small arrows in A and B) and by a straightening of the synaptic membranes and widening of the extrasynaptic space seen most clearly in C (arrowheads). In D, the synaptic specialization is no longer present. (E–G). A small symmetric ChAT synapse is clearly identifiable in only one serial section (arrowheads in F). In E, there is the suggestion of the beginnings of a membrane specialization. In F, the straightening and densification of the membranes become sufficient to identify the synapse. In addition, there is a small cluster of presynaptic vesicles (small arrow), which is partially obscured by reaction product. In G, the membrane specialization is no longer present. Scale bar = 0.5 μm.

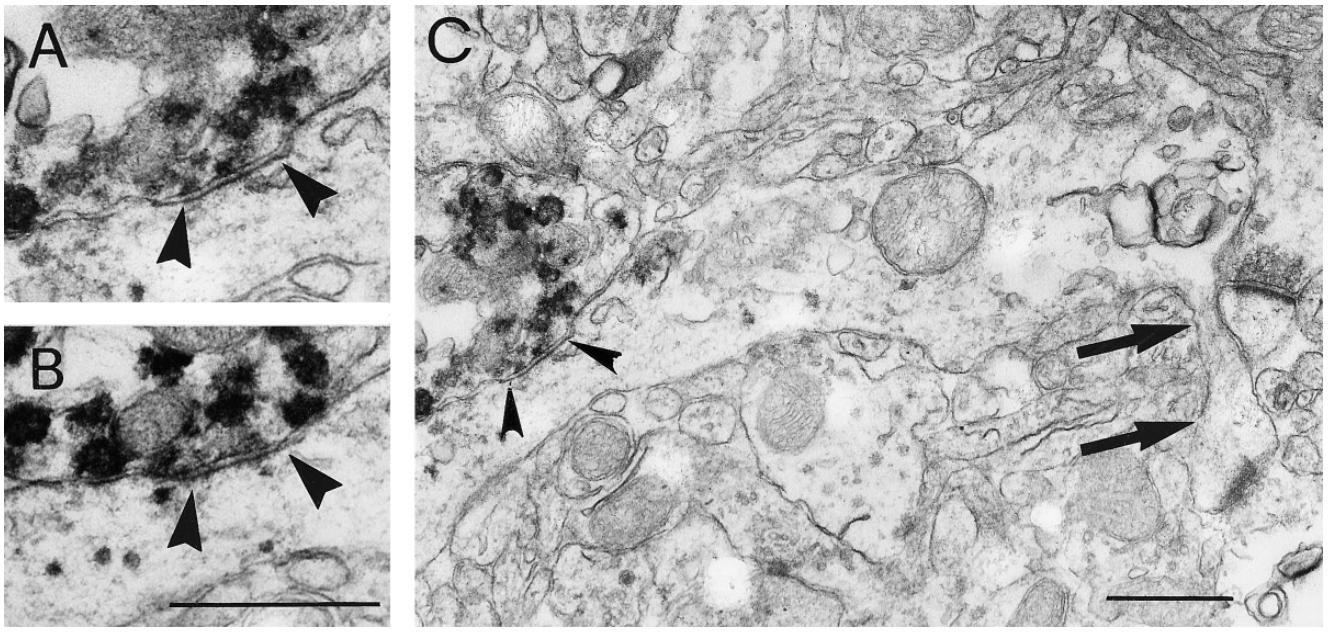

FIG. 5. Example of a cholinergic synapse (arrowheads) onto a spiny dendritic shaft. (A, B) This symmetric cholinergic synapse is seen in two adjacent serial sections. (C). At lower magnification of the same section shown in A, the postsynaptic dendrite is seen to form a large spine (arrows). Scale bars = 0.5 μm.

were apparent spine necks, having small diameters and prominent smooth endoplasmic reticulum (e.g., Fig. 3A). Because of their small diameter, only one of these was positively identified by following it to the spine head in serial sections. The symmetric and asymmetric synapses of ChAT axons were not distinguished by their postsynaptic targets, but instead each type was found on both dendritic spines and shafts.

When the two surgical samples were compared to each other, no significant differences were seen in the appearance of cholinergic axons or in the identity of the postsynaptic processes. The percentage of systematically surveyed varicosities forming identifiable synapses was 68% (15 of 22) in the first sample and 65% (13 of 20) in the second sample.

DISCUSSION

This study used samples of human cerebral cortex surgically removed from epileptic patients to demonstrate the ultrastructural features of ChAT-immunoreactive axons and their postsynaptic targets. The tissue samples analyzed for electron microscopy were chosen from regions with apparently normal cytoarchitectonics and ultrastructure. The results showed that ChAT-immunoreactive fibers in the human cerebral cortex were fine and unmyelinated and that they formed numerous varicosities, most of which gave rise to small symmetric synapses. The recipients of cholinergic synapses were predominantly dendritic spines or spiny dendritic shafts.

The finding that most cholinergic axon varicosities formed identifiable synapses contrasts with a recent study in the parietal cortex of the rat, which concluded that only 15% of cholinergic varicosities formed synapses (26). This low incidence of synaptic specializations in rat cortex was interpreted as a possible indicator that cholinergic axons rely heavily on volume transmission. Our results suggest that human cholinergic axons might rely more heavily on conventional synapses than in the rat. We were able to verify synaptic specializations on 67% of cholinergic varicosities, and the observation that many of these synapses were very small, seen in only one or two serial sections, raises the possibility that this may be an underestimation.

In many respects the ultrastructural appearance of cholinergic axons and their synaptic targets in human cortex is similar to what has been reported in the cerebral cortex, striatum, and thalamus of other species (1–7, 11, 23, 26, 28). Almost all of these studies reported unmyelinated axons with many vesicle-filled varicosities which usually form fine symmetric but sometimes asymmetric synapses. Two studies, one in the thalamus and the other in the hippocampus, suggested that the asymmetric synapses have different postsynaptic targets compared to symmetric synapses (6, 23). In the thalamus, asymmetric synapses were found preferentially on interneurons and symmetric synapses on relay cells (23). In the hippocampus asymmetric synapses preferentially targeted small spines, whereas symmetric synapses were found on large spines and dendritic shafts (6). The latter type of specificity

was not reported in rat neocortex or striatum. The present study found asymmetric and symmetric synapses on both spines and shafts, but the small sample prevents conclusions about a preferential distribution. While the physiological significance of synapse type is speculative, one possibility is that asymmetric synapses utilize a different type of acetylcholine receptor than symmetric synapses.

Similar to the present findings in the human, previous studies in monkey prefrontal cortex and in the rat dentate gyrus also reported an occasional dense core vesicle in cholinergic axons (4, 20). These were not mentioned in most studies in rats and cat, either because they were absent or because they might have been obscured by the immunocytochemical labeling. The functional significance of dense core vesicles is not precisely known, although they are often associated with the presence of neuropeptides (14). The identity of putative neuropeptides localized within cortical cholinergic axons remains unknown.

The postsynaptic targets of cholinergic synapses in human cortex were comparable to those in the cerebral cortex of other species. Previous studies in the cerebral cortex of rat, cat, and monkey reported that approximately 65–85% of cholinergic synapses were onto dendritic shafts, many of which were spiny (1, 2, 4–6, 11, 26, 28). The remaining postsynaptic processes were described as dendritic spines and, rarely, cell somas. We found 71% of cholinergic synapses to be on dendritic shafts, some of which were spiny. The remainder were onto small processes which had the appearance of spines and which were identified as the heads and necks of spines in a few cases. Because most cortical spines belong to pyramidal cells (21), these results suggest that most of the cholinergic synapses in human cerebral cortex are onto pyramidal cells. In other species, a minority of cholinergic synapses were found on dendrites of interneurons, as identified either by morphological features or GABA immunocytochemistry (2, 5, 11, 13, 20). We also noted occasional cholinergic synapses onto apparently nonspiny dendrites with a high density of synaptic inputs, an appearance that is characteristic of GABAergic interneurons in other species.

Electrophysiological studies in the cortex of cats and rodents have revealed several outcomes of cholinergic neurotransmission. These include the direct excitation of pyramidal cells and GABAergic interneurons and the indirect, perhaps presynaptic, modulation of GABAergic and glutamatergic transmitter release from axon terminals (9, 15, 18, 22, 27, 29, 30). Our findings in human cortex suggest that identifiable cholinergic synapses contact pyramidal cells and perhaps also interneurons. The observation that most cholinergic varicosities form synaptic contacts indicates that conventional synapses may account for a significant fraction of cholinergic neurotransmission in the human cerebral cortex, an arrangement that may differ from the one in the rat, where substantially fewer varicosities were reported to form synapses (26). Our results do not necessarily exclude the presence of volume transmission in the human cerebral cortex. For example, our unpublished observations in these same cortical samples demonstrated muscarinic receptor immunoreactivity in apparent glutamatergic axon terminals. A similar phenomenon has been observed in monkey cortex (19) and rat striatum (10). Since these glutamatergic axons lack identifiable axoaxonic synapses, cholinergic, or otherwise, the muscarinic receptors they contain are likely to represent heteroreceptors, the activation of which would depend on the volume transmission of acetylcholine.

This study provides the first ultrastructural evidence for the existence of synaptic cholinergic neurotransmission in the human cerebral cortex. The diversity of synaptic morphology and postsynaptic targets that we identified sets the stage for further studies on the pharmacological and physiological characteristics of cholinergic pathways in the human brain.

ACKNOWLEDGMENT

Supported by NS20285.

REFERENCES

1. Aoki, C., and S. Kabak. 1992. Cholinergic terminals in the cat visual cortex: Ultrastructural basis for interactions with glutamate-immunoreactive neurons and other cells. *Vis. Neurosci.* **8:** 177–191.
2. Beaulieu, C. and P. Somogyi. 1991. Enrichment of cholinergic synaptic terminals on GABAergic neurons and coexistence of immunoreactive GABA and choline acetyltransferase in the same synaptic terminals in the striate cortex of the cat. *J. Comp. Neurol.* **304:** 666–680.
3. Carlsen, J. and L. Heimer. 1986. A correlated light and electron microscopic immunocytochemical study of cholinergic terminals and neurons in the rat amygdaloid body with special emphasis on the basolateral amygdaloid nucleus. *J. Comp. Neurol.* **244:** 121–136.
4. Clarke, D. J. 1985. Cholinergic innervation of the rat dentate gyrus: An immunocytochemical and electron microscopic study. *Brain Res.* **360:** 349–354.
5. De Lima, A. D., and W. Singer. 1986. Cholinergic innervation of the cat striate cortex: A choline acetyltransferase immunocytochemical analysis. *J. Comp. Neurol.* **250:** 324–338.
6. Frotscher, M., and C. Leranth. 1986. The cholinergic innervation of the rat fascia dentata: Identification of target structures on granule cells by combining choline acetyltransferase immunocytochemistry and Golgi impregnation. *J. Comp. Neurol.* **243:** 58–70.
7. Frotscher, M., and C. Leranth. 1985. Cholinergic innervation of the rat hippocampus as revealed by choline acetyltransferase immunocytochemistry: A combined light and electron microscopic study. *J. Comp. Neurol.* **239:** 237–246.
8. German, D., G. Bruce, and L. B. Hersh. 1985. Immunohisto-

chemical staining of cholinergic neurons in the human brain using a polyclonal antibody to human choline acetyltransferase. *Neurosci. Lett.* **61:** 1–5.

9. Hasselmo, M. E., and J. M. Bower. 1992. Cholinegic suppression specific to intrinsic not afferent fiber synapses in rat prirofrm (olfactory) cortex. *J. Neurophys.* **67:** 1222–1229.
10. Hersch, S. M., C. A. Gutekunst, H. D. Rees, C. J. Heilman, and A. I. Levey. 1994. Distribution of m1–m4 muscarinic receptor proteins in the rat striatum: Light and electron microscopic immunocytochemistry using subtype-specific antibodies. *J. Neurosci.* **14:** 3351–3363.
11. Houser, C. R., G. D. Crawford, P. M. Salvaterra, and J. E. Vaughn. 1985. Immunocytochemical localization of choline acetyltransferase in rat cerebral cortex: A study of cholinergic neurons and synapses. *J. Comp. Neurol.* **234:** 17–34.
12. Hsu, S. M., L. Raine, and H. Fanger. 1981. Use of avidin–biotin–peroxidase complex (ABC) in immunoperoxidase techniques: A comparison between ABC and unlabeled antibody (PAP) procedures. *J. Histochem. Cytochem.* **29:** 577–580.
13. Leranth, C., and M. Frotscher. 1987. Cholinergic innervation of hippocampal GAD- and somatostatin-immunoreactive commissural neurons. *J. Comp. Neurol.* **261:** 33–47.
14. Matteoli, M., A. Reetz, and P. Decamilli. 1991. Small synaptic vesicles and large dense-core vesicles: Secretory organelles involved in two modes of neuronal signaling. In *Volume Transmission in the Brain* (K. Fuxe and L. F. Agnati, Eds.), pp. 181–193. Raven, New York.
15. McCormick, D. A., and D. A. Prince. 1986. Mechanisms of action of acetylcholine in the guinea-pig cerebral cortex in vitro. *J. Physiol.* **375:** 169–194.
16. Mesulam, M.-M., and C. Geula. 1993. Chemoarchitectonics of axonal and perikaryal acetylcholinesterase along information processing systems of the human cerebral cortex. *Brain Res. Bull.* **33:** 137–153.
17. Mesulam, M.-M., E. J. Mufson, and B. H. Wainer. 1986. Three-dimensional representation and cortical projection topography of the nucleus basalis (Ch4) in the macaque: Concurrent demonstration of choline acetyltransferase and retrograde transport with a stabilized tetramethylbenzidine method for horseradish peroxidase. *Brain Res.* **367:** 301–308.
18. Metherate, R., and J. H. Ashe. 1995. Synaptic interactions involving acetylcholine, glutamate, and GABA in rat auditory cortex. *Exp. Brain Res.* **107:** 59–72.
19. Mrzljak, L., A. I. Levey, and P. S. Goldman-Rakic. 1993. Association of m1 and m2 muscarinic receptor proteins with asymmetric synapses in the primate cerebral cortex: Morphological evidence for cholinergic modulation of excitatory neurotransmission. *Proc. Natl. Acad. Sci. USA* **90:** 5194–5198.
20. Mrzljak, L., M. Pappy, C. Leranth, and P. S. Goldman-Rakic. 1995. Cholinergic synaptic circuitry in the macaque prefrontal cortex. *J. Comp. Neurol.* **357:** 603–617.
21. Peters, A., S. L. Palay, and H. D. Webster. 1991. *The Fine Structure of the Nervous System*. Oxford Univ. Press, New York.
22. Pitler, T. A., and B. E. Alger. 1992. Cholinergic excitation of GABAergic interneurons in the rat hippocampal slice. *J. Physiol.* **450:** 127–142.
23. Schwartz, M. L., and L. Mrzljak. 1993. Cholinergic innervation of the mediodorsal thalamic nucleus in the monkey: Ultrastructural evidence supportive of functional diversity. *J. Comp. Neurol.* **327:** 48–62.
24. Smiley, J. F., and P. S. Goldman-Rakic. 1993. Heterogeneous targets of dopamine synapses in monkey prefrontal cortex demonstrated by serial section electron microscopy: A laminar analysis using the silver enhanced diaminobenzidine-sulfide (SEDS) immunolabeling technique. *Cerebral cortex* **3:** 223–238.
25. Smiley, J. F., and P. S. Goldman-Rakic. 1996. Serotonergic axons in monkey prefrontal cerebral cortex synapse predominantly on interneurons as demonstrated by serial section electron microscopy. *J. Comp. Neurol.* **367:** 431–443.
26. Umbriaco, D., K. C. Watins, L. Descarries, C. Cozzari, and B. K. Hartman. 1994. Ultrastructural and morphometric features of the acetylcholine innervation in adult rat parietal cortex: An electron microscopic study in serial sections. *J. Comp. Neurol.* **348:** 351–373.
27. Vidal, C., and J.-P. Changeuq. 1993. Nicotinic and muscarinic modulations of excitatory synaptic transmission in the rat prefrontal cortex in vitro. *Neuroscience* **56:** 23–32.
28. Wainer, B. H., J. P. Bolam, T. F. Freund, Z. Henderson, S. Totterdell, and A. D. Smith. 1984. Cholinergic synapses in the rat brain: A correlated light and electron microscopic immunohistochemical study employing a monoclonal antibody against choline acetyltransferase. *Brain Res.* **308:** 69–76.
29. Williams, S., and D. Johnston. 1990. Muscarinic depression of synaptic transmission at the hippocampal mossy fiber synapse. *J. Neurophys.* **64:** 1089–1097.
30. Williams, S. H., and D. Johnston. 1993. Muscarinic cholinergic inhibition of glutamatergic transmission. In *Presynaptic Receptors in the Mammalian Brain* (T. V. Dunwiddie and D. M. Lovinger, Eds.), pp. 27–41. Birkhauser, Boston.
31. Zhou, M., I. Grafova, and D. Tanaka. 1994. The use of peroxidase substrate VIP in EM double antigen location. *Soc. Neurosci. Abstr.* **20:** 703.